The FePt $L1_0$ Phase Transformation in Thin Films using Multiple Laser Pulsing

Gregory B. Thompson – The University of Alabama
et al.

Citation of published version:

Inaba, Y., et al. (2010): The FePt L10 Phase Transformation in Thin Films using Multiple Laser Pulsing. *Journal of Applied Physics*, 107(5).
DOI: https://doi.org/10.1063/1.3318492

The FePt $L1_0$ phase transformation in thin films using multiple laser pulsing

Yuki Inaba,[1] Gregory B. Thompson,[2,a)] J. W. Harrell,[3] Tim Klemmer,[4] and Yukiko Kubota[4]
[1]*Center for Materials and Information Technology, The University of Alabama, Tuscaloosa, Alabama 35487, USA*
[2]*Department of Metallurgical and Materials Engineering, The University of Alabama, Tuscaloosa, Alabama 35487, USA*
[3]*Department of Physics and Astronomy, The University of Alabama, Tuscaloosa, Alabama 35487, USA*
[4]*Seagate Technologies, Fremont, California 94538, USA*

(Received 14 October 2009; accepted 18 January 2010; published online 4 March 2010)

A series of ≈12 nm thick FePt thin films deposited onto glass substrates have been annealed with multiple 1064 nm wavelength laser pulses. The fluence was varied using pulse widths of 10.0, 5.0, and 2.5 ms. The peak temperature for each individual pulse was kept near 700 °C. The A1 to $L1_0$ phase transformation was confirmed by x-ray diffraction. A single pulse was not sufficient to obtain a fully ordered state. A maximum order parameter of 0.89 and coercivity of 10.6 kOe was obtained after 5×10 ms pulses. This particular annealed film showed the greatest amount of grain growth with a mean size of 55.1 nm. This grain size is 20% smaller than that of a furnace annealed sample which was annealed for 60 s and yielded an approximately equivalent order parameter. Similar order parameters, grain sizes, and coercivity values were observed for films that had equivalent total annealing times regardless of pulse widths. © *2010 American Institute of Physics*.
[doi:10.1063/1.3318492]

I. INTRODUCTION

The high magnetocrystalline anisotropy, K_u, of $L1_0$ FePt ($\sim7\times10^7$ ergs/cc) has made this material a candidate for future ultrahigh density perpendicular magnetic recording.[1,2] When this alloy is sputter-deposited as a thin film, it nominally adopts a metastable, high temperature A1 phase. A subsequent anneal greater than approximately 500 °C (Refs. 3 and 4) will phase transform the FePt film into the thermodynamically stable, magnetically hard $L1_0$ phase. During annealing, grain coarsening results and broadens the grain size distribution, which is detrimental for ultrahigh density storage applications.[5,6]

Recent theoretical modeling predictions have suggested that the A1 to $L1_0$ ordering reaction occurs in the tens to hundreds of milliseconds regime for annealing temperatures of 500–1000 °C.[7,8] Though the time scale predictions are based on micron-scale thicknesses, and thinner films can experience delayed ordering,[8] these predicted time scales would provide the shortest times where ordering could be initiated. If anything, experimental validation of ordering in a thinner film, where delayed ordering could occur, would validate these millisecond scale annealing predictions. An intriguing question is whether detrimental grain growth can be eliminated or significantly reduced if ordering can be initiated in the millisecond time regime.

One of the experimental challenges to probe this time-temperature regime is the ability to rapidly heat and cool the specimens at these short times. There have been some reports using conventional rapid thermal annealing techniques,[9–12] but these time scales are in seconds to tens of seconds, which are orders of magnitude too long for the proposed minimum time scales for ordering. Pulse laser annealing could provide an alternative with shorter annealing times. Buschbeck *et al.*[13] have used laser annealing techniques but the pulse widths were in the nanosecond regime, which are several orders of magnitude too fast to allow sufficient atomic diffusion.

We have recently shown that laser annealing by single laser pulses with pulse widths up to 10 ms can be sufficient to facilitate FePt $L1_0$ ordering;[14] however, the maximum order parameter was small compared to that obtained for longer conventional furnace annealing times. Most recently, we have shown that multiple pulse processing using a plasma processing lamp can be used to achieve higher order parameters while minimizing grain growth.[15] In this paper, we have explored multiple laser pulsing to determine if similar effects can be achieved. In addition, our previous paper on laser pulsing[14] reported the single pulse experiments in terms of laser fluence; the current work provides a means to quantify the temperature during each pulse. From the multiple thermal laser exposures, the relationship between order parameter and grain growth is reported.

II. EXPERIMENTAL PROCEDURE

An ≈12 nm thick FePt thin film was deposited onto a Corning 1737 2 –in., square glass substrate by dc (direct current) sputtering from 99.5% elemental Fe and Pt targets in an AJA ATC-1500 magnetron sputtering system. The base pressure was $<5\times10^{-8}$ Torr prior to sputtering at which point ultrahigh-purity Ar was flowed at 10 SCCM (standard cubic centimeters per minute) into the chamber to a pressure of 2 mTorr. The films consisted of the multilayer structure Si_3N_4 (5 nm)/[Fe (~0.24 nm)/Pt(~0.3 nm)]$_{22}$/Si_3N_4 (5 nm)/

a)Electronic mail: gthompson@eng.ua.edu.

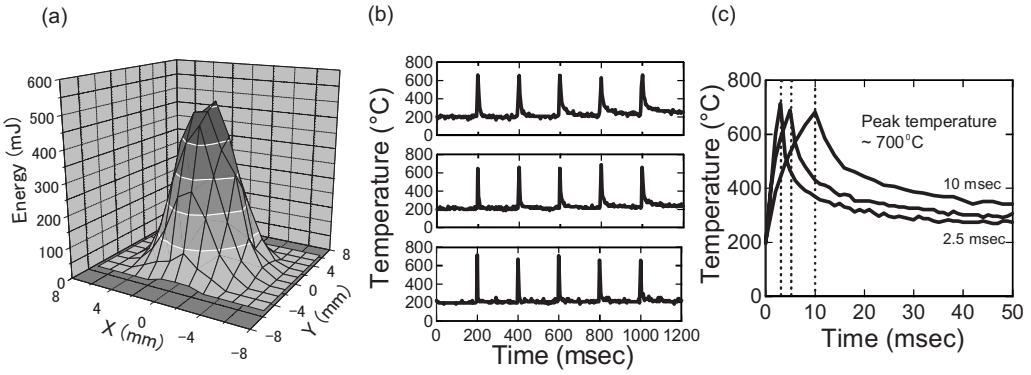

FIG. 1. (a) 3D laser intensity profile and (b) time-temperature profile for five applied pulses with various pulse widths and (c) time-temperature profile for a single pulse at different pulse widths.

glass substrate. The subscript "22" represents the number of Fe/Pt bilayers deposited prior to the Si_3N_4 capping layering. The Fe and Pt thicknesses were determined by the sputtering rate and time each sputtering gun shutter was open, and is similar to the ratio of Fe/Pt thicknesses reported by Yao and Coffey[16] for yielding equiatomic mixing. Since the thickness of the film only varies (constant cross sectional area), the number of Fe and Pt moles for these thicknesses would be 50/50, assuming the molar volume of Fe is 7.9 cm^3/mole and Pt is 9.09 cm^3/mole. The equiatomic composition was confirmed by scanning transmission electron microscopy-x-ray energy dispersive spectroscopy (STEM-XEDS) analysis. The Cliff–Lormer k-factor for XEDS quantification was verified using a homogeneous FePt thin film whose composition was verified by Rutherford backscattering.[17] In addition, atom probe tomography studies of similar multilayered films have shown that these very thin individual layers are highly intermixed in the as-deposited state and yield a near equiatomic composition of FePt.[18] It should be noted that depositing the FePt film as a series of very thin individual layers may facilitate faster ordering, as reported in other systems.[19,20]

A Si_3N_4 composite target was used to grow the Si_3N_4 layers by rf (radio frequency) sputtering. The Si_3N_4 acts as a diffusion barrier to prevent any undesired substrate or atmospheric reactions with the FePt thin film during annealing.[15] Post deposition, the wafer was diced into 5 mm × 5 mm squares for the laser and furnace annealing studies.

An Electrox Scorpion Nd-YAG laser with a wavelength of 1064 nm was used to anneal the thin film specimens. The specimens were placed in a Corning MACOR Machineable Glass Ceramic holder which had a hole through the center. The hole minimized the contact to <0.5 mm at the edges of the specimen which reduced thermal contact with the mount.

In order to anneal the film with the laser, the 5 mm square specimens were placed approximately 40 mm from the focus. The laser beam intensity profile at this distance was measured using a 1 mm aperture and a power meter. The profile was approximately Gaussian in shape, as shown in Fig. 1(a). The intensity deviated approximately 20% across the 5 mm square sample from peak to the edge.

The specimens were annealed in air using laser pulses with pulse widths of 10.0, 5.0, or 2.5 ms. For pulse widths of 2.5 ms, the applied pulses were varied in steps of one from 1 to 10. For pulse widths of 5.0 and 10.0 ms, the number of applied pulses was varied in steps of one from 1 to 5. The time between consecutive pulses was 200 ms. This 200 ms interval was found to provide sufficient cooling back to the base temperature prior to the subsequent pulse. The pulse width was controlled by a mechanical shutter in the laser. From a previous single pulse laser annealing study,[14] it was found that there was an optimum delivered laser fluence for each pulse width to obtain the FePt $L1_0$ phase transformation. In this study, this optimum delivered laser fluence was chosen and carefully optimized to ensure that each pulse generated the same peak temperature during each pulse sequence. To minimize potential delamination or thermal shock because of thermal expansion differences between the film and the substrate during the laser pulse, the specimens were preheated at a temperature of 200 °C using a quartz lamp positioned under the ceramic mount. This preheat temperature is below the A1 to $L1_0$ ordering temperature.[8]

For microstructure comparisons to the laser annealed thin films, representative specimens from the same wafer were annealed for 60 s at the set-point temperature from 400 to 800 °C at 100 °C increments in a conventional tube furnace. The heating rate was dependent upon the set-point temperature. For example, it took 480 s to achieve 400 °C (0.83 °C/s), 300 s for 600 °C (2.00 °C/s), and 220 s for 800 °C (3.63 °C/s). Once the set point was achieved, the specimen was held for 60 s and then removed from the furnace. The cooling rates were also temperature dependent but, in general, it took approximately 20 min to reach room temperature for each specimen.

A Raytek MARATHON MM 2ML optical pyrometer was used to provide qualitative measurements of the temperature rise and fall on the specimen during the laser pulse. The pyrometer has a time constant of 2 ms (95% recovery), which yields an adequate time scale resolution for the annealing times investigated. To calibrate the temperature, it is necessary to know the relationships between laser fluence and film temperature. This was measured by depositing a ≈12 nm Pt thin film sandwiched between two 5 nm Si_3N_4 films on the glass substrate to prevent reactions with either the substrate or atmosphere. The Pt film acts as a thin film resistor. To improve the reproducibility and linearity of the temperature dependence of the resistance, the film was pre-

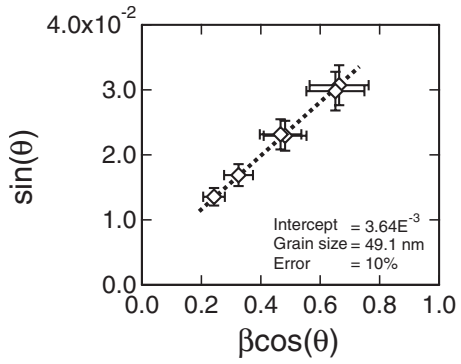

FIG. 2. An example of a Williamson–Hall plot obtained from the 5 $\times 10$ ms annealed FePt specimen. Here, theta, θ, is peak angle obtained from XRD and β is the peak width. The data were obtained from the (110), (220), (202), (001), (002), and (200) reflections. Since there is some error in separating closely separated peaks, such as (220) and (202), theta for such peaks contain a larger error as compared to peaks where separation is not problematic, such as (110).

annealed at 600 °C for 3 h to facilitate grain growth. The resistance of the Pt thin film was measured as a function of temperature using static temperature measurements collected while annealing the film in a tube furnace. The resistance changed linearly with changes in temperature. Subsequently, the resistance change of the Pt thin film was measured and recorded during the laser pulse using an oscilloscope with various laser fluences. Using this resistance data, the temperature dependence on laser fluence was obtained. The real and imaginary parts of the index of refraction of Pt and FePt at 1064 nm are very similar. For Pt, n=3.67 and k=5.94,[21] and for FePt, n≈3.6 and k≈5.0.[22] The laser absorptions calculated using these values are nearly the same.[23] Likewise, the thermal properties (volume heat capacity, thermal conductivity, and thermal diffusivity) are very similar.[13,24,25] Thus, the temperature response to the laser pulses is expected to be nearly the same in Pt and FePt thin films. The resistance of the FePt film was deemed unsuitable for direct measurement of the temperature since resistance changes would be expected to be accompanied by grain growth and the $L1_0$ phase change.

The transmission electron microscopy (TEM) analysis was performed using a 200 keV Field Emission FEI Tecnai F20 Supertwin TEM. TEM foils were prepared by standard polishing, backside dimpling, and ion milling. X-ray diffraction (XRD) spectra were collected using a Bruker D8 Discovery general area diffraction detection system using Co $K\alpha$ radiation ($\lambda=1.789$ Å) as the source. In addition, a Philips x-ray diffractometer using Cu $K\alpha$ radiation ($\lambda=1.540$ Å) as the source was used. The specimens were tilted 88° so that the XRD diffracted vector was nearly in-the-plane for the grain size analysis. The grain size (crystallite size) was determined by the Williamson–Hall plot[26] using several peaks from the in-plane XRD measurements. An example of such a plot can be viewed in Fig. 2. The order parameter, S, was determined by XRD using the equation[27]

$$S^2 = \frac{(I_{110}/I_{220})_{\exp}}{(I_{110}/I_{220})_{calc}}. \quad (1)$$

The calculated ratio of x-ray intensities for the (110) and (220) reflections were obtained using the JCPDS index card #00–043–1359. Since the films exhibited a strong (111) texture, the specimens were tilted 35.2°, the angle between the [111] and [110] directions, which allowed the experimental superlattice reflections, and their corresponding intensities, to be easily observed and quantified in the XRD spectra.

In-plane hysteresis loops were measured with a Princeton Instruments Model 2900 alternating gradient magnetometer (AGM) with a maximum applied field of 18 kOe. The limited field of the AGM was, in some films, insufficient to fully saturate the film, making the coercivity values reported an underestimation.

III. RESULTS AND DISCUSSION

The time-temperature profile for 5 pulses with each pulse width being 10.0, 5.0, and 2.5 ms showed a peak temperature around 700 °C, as seen in Fig. 1(b). The laser fluence was adjusted such that the same peak temperature for each pulse was successfully obtained throughout the annealing process and the pulse interval allowed the film to cool to its preheat temperature after each pulse. The peak temperature occurred at the end of each pulse, as seen in Fig. 1(c).

The in-plane hysteresis loops for the samples annealed with 10.0, 5.0, and 2.5 ms pulse widths and 1, 3, and 5 applied pulses is plotted in Figs. 3(a)–3(c). The loops for the as-deposited and 700 °C furnace annealed samples are also shown for comparison. Note that the 700 °C furnace annealed sample is nearly the same temperature as the peak temperature achieved via laser annealing. Figure 4 shows the coercivity, H_c, dependence on the number of applied pulses

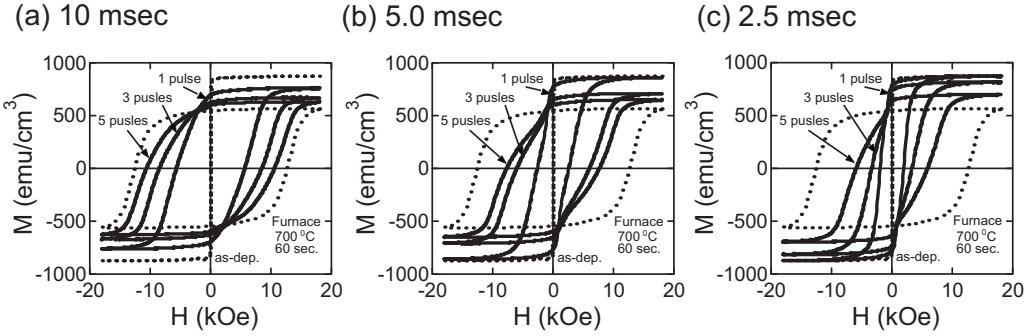

FIG. 3. In-plane hysteresis loops of films annealed with pulse widths of (a) 10.0 ms, (b) 5.0 ms, and (c) 2.5 ms. The number of applied pulses is 1, 3, and 5. The hysteresis loops for as-deposited and furnace annealed sample (700 °C, 60 s) are also shown for comparison.

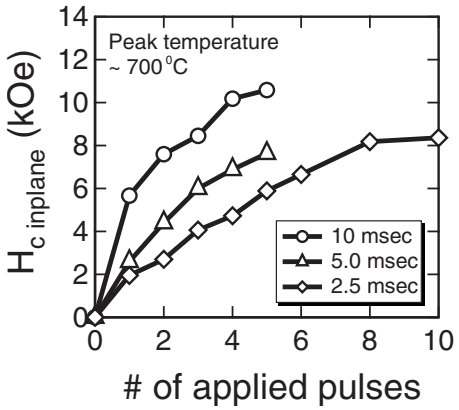

FIG. 4. Coercivity dependence on number of applied pulses. Peak temperature was approximately 700 °C.

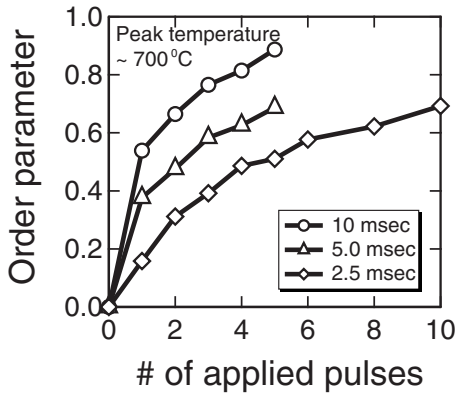

FIG. 6. Order parameter dependence on number of applied pulses. Peak temperature was around 700 °C.

for the various pulse widths. The number "0" corresponded to the as-deposited state and its coercivity was nearly zero, consistent with the magnetically soft A1 phase. As the number of applied pulses increased, H_c increased. A large H_c was obtained even at one 2.5 ms pulse, as plotted in Fig. 4. This suggested that 2.5 ms for 700 °C is not the lower time bound necessary to initiate ordering at this temperature. H_c also increased as the pulse width increased. The hysteresis loops that gave the maximum H_c were not fully saturated with the maximum AGM applied field of 18 kOe, as indicated by the drop in the saturation magnetization seen in Fig. 3. The general shape of the loops also suggests the presence of both hard and soft phases. The existence of two phases indicates that not all the material has phase transformed to $L1_0$ or that the local average degree of order is not the same over the sample. The multiple phases may be because the delivered energy density is not uniform across the film surface, as shown in Fig. 1(a), which could prevent uniform transformation.

The out-of-plane XRD spectrum for the 10 ms pulse width with various numbers of applied pulses is plotted in Fig. 5(a). The film showed strong (111) orientation parallel to the growth direction in the as-deposited state. After annealing, this (111) peak shifted toward a larger 2θ angle consistent with $L1_0$ chemical ordering. The intensity of the (110) super-lattice peak, indicative of $L1_0$ ordering, increased as the number of applied pulses increased, as seen in Fig. 5(b).

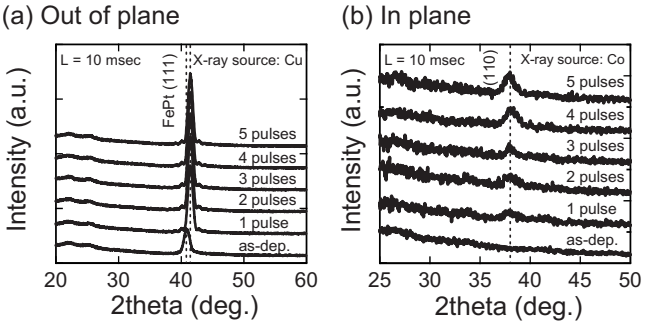

FIG. 5. (a) Out-of-plane XRD profile and (b) In-plane XRD profile of samples annealed with 10 ms laser pulse width. The numbers of applied pulses are 1, 2, 3, 4, and 5.

The increase in this superlattice reflection is consistent with the H_c increase, as seen in Fig. 4. This trend was the same for the other pulse widths.

The increase in the superlattice reflection intensity indicated that the average order parameter, S, increased with either longer pulse widths and/or number of applied pulses, as plotted in Fig. 6. This trend is similar to that observed for H_c in Fig. 5. Ristau *et al.*[28] has reported that coercivity increased with increasing FePt ordered volume fraction; at 700 °C, an ordered fraction of near unity can take more than 100 min.[28] For clarity, this paper has addressed order parameter, not ordered fraction. The increasing trend of H_c, Fig. 5, is likely a combination of increasing order parameter, Fig. 6, and ordered volume fraction[28] with each laser pulse. For the same number of pulses, S was larger for pulses that had a longer pulse width. An order parameter near $\approx$0.9 was only achieved for the longest pulse width of 10 ms and required five consecutive pulses.

The average XRD determined grain size, $\langle D \rangle$, dependence on the number of applied pulses is plotted in Fig. 7. A plan-view TEM image was taken from the as-deposited film which confirmed close agreement of the average grain sizes between the XRD estimation, 22.9 nm, and TEM image, 23.6 nm.[14] The grain size increased as the number of applied pulses increased for all pulse widths. For a fixed number of pulses, the grain size also increased with increasing pulse width. Ristau *et al.*[9] has shown that FePt grain growth pro-

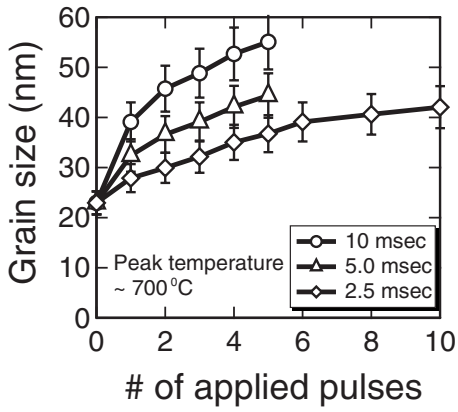

FIG. 7. Grain size dependence on number of applied pulses. Peak temperature was around 700 °C. The error bar represented is 1σ.

TABLE I. Order parameter and the mean grain size of three different pulse widths but equivalent total annealing time.

Condition	10 ms×1 pulse	5.0 ms×2 pulses	2.5 ms×4 pulses
Order parameter	0.54	0.50	0.48
Coercivity (kOe)	5.67	4.60	4.73
Grain size (nm)	39.1	36.6	35.0

ceeds rapidly before any substantial phase transformation has occurred. Once grain growth slowed, the ordering reaction progressed rapidly. In their work,[9] the initial film was 10 nm thick with an in-plane grain size of ≈6 nm. Upon a conventional tube furnace anneal at 700 °C for 120 min (10 min heating rate to achieve the set point), the grains grew to ≈32 nm. Though this final grain size is less than the final grain sizes reported in this paper, the grain growth for Ristau *et al.*[9] was nearly 5× where as the pulsed laser annealed films grew from ≈23 nm to ≈50 nm, or 2× increase. Comparing Ristau *et al.*'s Ref. 9 to Ref. 28 reveals that these films, after 120 min of annealing at 700 °C, had an ordered fraction of greater than 0.9. Achieving order quickly appears to be a critical step in reducing grain growth. The $L1_0$ phase has three possible *c*-axis variants,[3] which can lead to antiphase boundaries and other similar ordered phase interfacial energy penalties that can inhibit grain growth. This may explain the slower grain growth observed in the ordered films.[2]

An interesting question is whether H_c, S, and $\langle D \rangle$ depend on total pulse time or on the individual pulse widths for a given total time. Table I gives S, H_c, and $\langle D \rangle$ for a total annealing time of 10 ms obtained with one 10 ms pulse, two 5 ms pulses, and four 2.5 ms pulses. The values of S, H_c, and $\langle D \rangle$ are nearly the same for the 2.5 and 5 ms pulses and are slightly larger for the 10 ms pulse. These differences may be because of differences in the effective annealing times. The effective anneal time is not necessarily the same as the laser pulse width because of the complex time-temperature profile and the nonlinear dependence of ordering on temperature. The time-temperature profiles, as seen in Fig. 1, exhibited a slight difference in the temperature rise and cool-down dependent on the pulse width and heating of the film and substrate. This effective heating/cooling difference likely contributed to the deviations measured in S, H_c, and $\langle D \rangle$.

The order parameter dependence on average grain size is plotted in Fig. 8. In this figure, the data obtained with the furnace annealed films are also shown for comparison. For both the laser annealed and furnace annealed films, the order parameter increased with grain size. This order parameter rate of increase, however, is significantly more for the laser annealed films, which suggested that millisecond time annealing does indeed reduce grain growth. In addition, there is a slight reduction in grain growth as the laser pulse width is reduced. The maximum S obtained with laser annealing was 0.89 using five 10 ms pulses, which resulted in a grain size of 55.1 nm. In contrast, the same order parameter could be obtained by furnace annealing at approximately 700 °C for 60 s which resulted in a grain size of 68.5 nm. In this work, chemically ordering appeared to be a relatively quick process

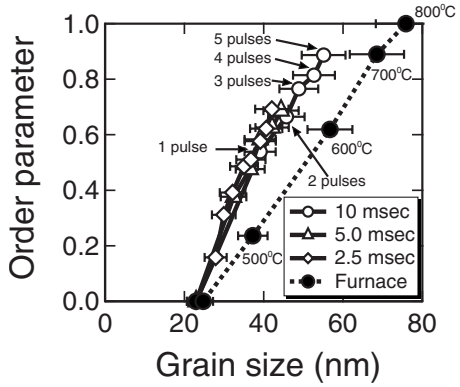

FIG. 8. Order parameter dependence on grain size. Data obtained with furnace annealing experiment with the furnace set point next to each datum. Increases in tube furnace temperature resulted in an increase in order parameter and grain size. Similar effects were observed with increasing the number of laser pulses applied for a fixed peak temperature at 700 °C; the arrows indicate the datum point for the number of 10 ms pulses applied. Similar trends of increasing order parameter with consecutive number of increasing pulses for the other pulse widths was observed, *i.e.*, the lowest order parameter corresponded to one pulse and the highest order parameter corresponded to highest number of applied pulses. Note that the grain size for the laser annealed films scaled with increasing number of pulses. The error bar represented is 1σ.

on the order of tens of milliseconds and excessive grain growth is continuous with longer and/or slower ramp rate annealing times.

IV. CONCLUSION

It has been shown that $L1_0$ chemical ordering can be obtained in FePt thin films using multiple millisecond laser pulses. These results provide experimental confirmation of the predicted time scales where ordering is initiated,[7,8] *i.e.* the millisecond regime. The degree of order, coercivity, and grain growth all increased with either an increase in laser pulse width and/or cumulative annealing time. S and H_c were nearly independent of pulse width for a fixed cumulative annealing time and depended primarily on the total time. In addition, a high degree of order (0.89) could be achieved with five 10 ms pulses with peak temperature of 700 °C. Grain growth in a continuous FePt thin film was not prevented using the laser annealing technique; however, grain growth decreased with decreasing pulse width and is less than that of longer annealing times in a conventional tube furnace. While application of single 10.0, 5.0, and 2.5 ms pulses was not sufficient to obtain a high degree of chemical order, the degree of order can be increased by using multiple pulses at these pulse widths.

ACKNOWLEDGMENTS

This research was supported by the Center for Materials for Information Technology at the University of Alabama through a grant by Seagate Technologies and made use of shared facilities under NSF Materials Research Science and Engineering Center Award No. DMR-0213985. G. B. Thompson acknowledges additional support from NSF-DMR-0529369. The authors gratefully acknowledge Professor Ramana Reddy for use of the Nd-YAG laser. The Tecnai TEM

was acquired through the National Science Foundation Major Instrumentation Program, NSF-DMR-0421376.

[1]B. Zhang and W. A. Soffa, Scr. Metall. **30**, 683 (1994).
[2]T. J. Klemmer, D. Hoydick, H. Okumura, B. Zhang, and W. A. Soffa, Scr. Metall. **33**, 1793 (1995).
[3]D. E. Laughlin, K. Srinivasan, M. Tanase, and L. Wang, Scr. Mater. **53**, 383 (2005).
[4]C.-M. Kuo, P. C. Kuo, and H.-C. Wu, J. Appl. Phys. **85**, 2264 (1999).
[5]H. Uwazumi, T. Shimatsu, Y. Sakai, A. Otsuki, I. Watanabe, H. Muraoka, and Y. Nakamura, IEEE Trans. Magn. **37**, 1595 (2001).
[6]K. Miura, H. Muraoka, Y. Sugita, and Y. Nakamura, J. Magn. Soc. Jpn. **24**, 231 (2000).
[7]B. Rellinghaus, E. Mohn, L. Schultz, T. Gemming, M. Acet, A. Kowalik, and B. F. Kock, IEEE Trans. Magn. **42**, 3048 (2006).
[8]D. C. Berry and K. Barmak, J. Appl. Phys. **101**, 014905 (2007).
[9]R. A. Ristau, K. Barmak, K. R. Coffey, and J. K. Howard, J. Mater. Res. **14**, 3263 (1999).
[10]S. Jeong, Y-.N. Hsu, D. E. Laughlin, and M. E. McHenry, IEEE Trans. Magn. **36**, 2336 (2000).
[11]Y. Shao, M. L. Yan, and D. J. Sellmyer, J. Appl. Phys. **93**, 8152 (2003).
[12]H. Zeng, S. Sun, R. L. Sandstrom, and C. B. Murray, J. Magn. Magn. Mater. **266**, 227 (2003).
[13]J. Buschbeck, S. Fähler, M. Weisheit, K. Leistner, J. McCord, B. Rellinghaus, and L. Schultz, J. Appl. Phys. **100**, 123901 (2006).
[14]Y. Inaba, S. Kang, J. R. Izatt, J. W. Harrell, G. B. Thompson, Y. Kubota, and T. J. Klemmer, J. Appl. Phys. **105**, 07B715 (2009).
[15]Y. Inaba, K. L. Torres, A. Cole, R. Vanfleet, R. Ott, T. Klemmer, J. W. Harrell, and G. B. Thompson, J. Magn. Magn. Mater. **321**, 2451 (2009).
[16]B. Yao and K. R. Coffey, J. Appl. Phys. **105**, 033901 (2009).
[17]C. Srivastava, D. E. Nikles, and G. B. Thompson, J. Appl. Phys. **104**, 064315 (2008).
[18]K. L. Torres and G. B. Thompson, Ultramicroscopy **109**, 606 (2009).
[19]T. Shima, T. Moriguchi, S. Mitani, and K. Takanashi, Appl. Phys. Lett. **80**, 288 (2002).
[20]T. Shima, T. Moriguchi, T. Seki, S. Mitani, and K. Takanashi, J. Appl. Phys. **93**, 7238 (2003).
[21]M. A. Ordal, L. L. Long, R. J. Bell, S. E. Bell, R. R. Bell, R. W. Alexander, and C. A. Ward, Appl. Opt. **22**, 1099 (1983).
[22]K. Sato, A. Mizusawa, K. Ishida, T. Shima, and K. Takanashi, Trans. Magn. Soc. Jpn. **4**, 297 (2004).
[23]O. S. Heavens, *Optical Properties of Thin Solid Films* (Butterworth, London, 1955), pp. 76–77.
[24]J. W. Arblaster, Platinum Met. Rev. **38**, 119 (1994).
[25]Y. Terada, K. Ohkubo, T. Mohri, and T. Suzuki, J. Alloys Compd. **285**, 233 (1999).
[26]G. K. Williamson and W. H. Hall, Acta Metall. **1**, 22 (1953).
[27]B. E. Warren, *X-Ray Diffraction* (Addison-Wesley, Reading, MA, 1969).
[28]R. A. Ristau, K. Barmak, L. H. Lewis, K. R. Coffey, and J. K. Howard, J. Appl. Phys. **86**, 4527 (1999).